Supplemental Material can be found at:
http://www.jbc.org/content/suppl/2012/08/28/M112.399410.DC1.html

THE JOURNAL OF BIOLOGICAL CHEMISTRY VOL. 287, NO. 44, pp. 36756–36765, October 26, 2012
© 2012 by The American Society for Biochemistry and Molecular Biology, Inc. Published in the U.S.A.

The Claudin Megatrachea Protein Complex*[S]

Received for publication, July 10, 2012, and in revised form, August 16, 2012 Published, JBC Papers in Press, August 28, 2012, DOI 10.1074/jbc.M112.399410

Martin H. J. Jaspers[‡1], Kai Nolde[‡1], Matthias Behr[§2], Seol-hee Joo[‡], Uwe Plessmann[¶], Miroslav Nikolov[¶3], Henning Urlaub[¶‖], and Reinhard Schuh[‡4]

From the [‡]Research Group Molecular Organogenesis, [¶]Bioanalytical Mass Spectrometry Group, Max Planck Institute for Biophysical Chemistry, Am Fassberg, 37077 Göttingen, Germany, [‖]Bioanalytics, Department of Clinical Chemistry, University Medical Center Göttingen, Robert-Koch-Strasse 40, 37075 Göttingen, Germany, and [§]Life and Medical Sciences Institute, University of Bonn, Carl-Troll-Strasse 31, 53115 Bonn, Germany

Background: Claudins mediate the trans-epithelial barrier function of epithelial tissues in vertebrates and invertebrates.
Results: Proteomic and *in vivo* analyses of the claudin Megatrachea protein complex identify novel Megatrachea interacting factors.
Conclusion: The claudin Megatrachea interacting factors include members of the clathrin-mediated endocytosis and a novel putative scavenger receptor.
Significance: This is a comprehensive analysis of a claudin interactome.

Claudins are integral transmembrane components of the tight junctions forming trans-epithelial barriers in many organs, such as the nervous system, lung, and epidermis. In *Drosophila* three claudins have been identified that are required for forming the tight junctions analogous structure, the septate junctions (SJs). The lack of claudins results in a disruption of SJ integrity leading to a breakdown of the trans-epithelial barrier and to disturbed epithelial morphogenesis. However, little is known about claudin partners for transport mechanisms and membrane organization. Here we present a comprehensive analysis of the claudin proteome in *Drosophila* by combining biochemical and physiological approaches. Using specific antibodies against the claudin Megatrachea for immunoprecipitation and mass spectrometry, we identified 142 proteins associated with Megatrachea in embryos. The Megatrachea interacting proteins were analyzed *in vivo* by tissue-specific knockdown of the corresponding genes using RNA interference. We identified known and novel putative SJ components, such as the gene product of *CG3921*. Furthermore, our data suggest that the control of secretion processes specific to SJs and dependent on Sec61p may involve Megatrachea interaction with Sec61 subunits. Also, our findings suggest that clathrin-coated vesicles may regulate Megatrachea turnover at the plasma membrane similar to human claudins. As claudins are conserved both in structure and function, our findings offer novel candidate proteins involved in the claudin interactome of vertebrates and invertebrates.

The main function of epithelial sheets is the establishment and maintenance of well defined fluid compartments in multicellular organisms by controlling the paracellular flow of water-soluble molecules between adjacent epithelial cells. This barrier function is mediated by membrane-anchored protein complexes, the tight junctions (TJs)[5] in vertebrates and the septate junctions (SJs) in invertebrates (1, 2). The TJs are localized laterally in the most apical plasma membrane of the polarized epithelial cell. They organize focal contacts between neighboring cells and thereby establish a barrier that controls the flow of solutes across the epithelium. In contrast, the SJs extend more basally in the lateral membranes and, based on the alternating appearance of porous and dense material between the lateral cell membranes of two adjacent cells, display a ladder-like structure in electron microscopic images (3–5).

Despite their different morphology, membrane localization, and functional properties both SJs and TJs contain members of the transmembrane claudin protein family (6, 7). Claudins were first identified in TJs from chicken liver cells, and so far 27 members have been identified in vertebrates (7, 8). Each claudin exhibits a distinct tissue-specific expression pattern, and it has been suggested that the levels and the combination of claudins are crucial in the regulation of the selectivity of the epithelial barrier function. Severe human diseases are caused by mutations in claudin genes, and various claudins are abnormally expressed in cancers (6). In contrast to vertebrates, the *Drosophila* claudins comprise a small group of only three proteins, Megatrachea (Mega) (9), Sinuous (10), and Kune-kune (Kune) (11). Lack-of-function and gain-of-function experiments revealed that the *Drosophila* claudins mediate the transepithelial barrier function as found for vertebrate claudins (9–11).

Claudins are characterized by four transmembrane domains, a large and a small extracellular loop, an intracellular loop, and N- and C-terminal cytoplasmic regions. Also, most of the claudin proteins contain potential protein-protein interaction domains, with which they may interact with the protein binding PDZ motifs of cytoplasmic proteins. For example, the PDZ domains of MUPP1 (multi-PDZ domain protein 1) are binding

* This work was supported by the Max-Planck-Society (MPIbpc Abt.11020).
[S] This article contains supplemental Tables 1 and 2 and Figs. 1 and 2.
[1] Both authors contributed equally to this work.
[2] Supported by the Deutsche Forschungsgemeinschaft (SFB645).
[3] Supported by a fellowship from the Ph.D. program "Molecular Biology," International Max Planck Research School at the Georg August University Göttingen.
[4] To whom correspondence should be addressed: Tel.: 495512011758; Fax: 495512011755; E-mail: rschuh@gwdg.de.

[5] The abbreviations used are: TJ, tight junction; SJ, septate junction; Mega, Megatrachea; LC, liquid clearance; Chc, clathrin heavy chain; IP, immunoprecipitation; mAb, monclonal antibody.

Downloaded from www.jbc.org at Max Planck Inst.Biophysikalische Chemie,Otto Hahn Bibl,Pf.2841,37018 Goettingen, on December 5, 2012

partners of claudin-1 (12) and claudin-5 (13). In addition, the TJ-associated MAGUKs (membrane-associated guanylate kinase-like homologues) ZO-1, ZO-2, and ZO-3 bind directly to the C termini of claudins (14). Furthermore, gain-of-function experiments suggest an interaction of the *Drosophila* claudin Mega with the Coracle (homologous to the human erythrocyte protein 4.1)-Neurexin protein complex of SJs (9). The important role of *Drosophila* claudins for SJ formation via protein-protein interactions is further supported by the observation that the lack of a particular claudin leads to the disintegration of SJs (9–11). In addition to claudins, an increasing number of SJ proteins have been identified in the last years (15, 16). However, no comprehensive study of the claudin interactome has been performed in invertebrates.

Here we show a proteomic analysis of the *Drosophila* embryonic claudin Mega interactome by immunoprecipitation and mass spectrometry. We identified 142 different proteins that potentially interact in a direct or indirect manner with the SJ protein Mega. Tissue-specific knockdown experiments of the corresponding genes by RNA interference and their phenotypic *in vivo* analysis revealed putative essential SJ components, factors that mediate secretion via Mega, and components involved in Mega turnover at the plasma membrane.

EXPERIMENTAL PROCEDURES

Isolation of Membrane Extracts from Drosophila Embryos—Wild-type *Drosophila* embryos (1g; 9–22 h old) were dechorionated with 2.5% sodium hypochlorite (commercial bleach diluted 1:1 with H_20) for 5 min at room temperature. All procedures beyond this point were carried out at 4 °C. Dechorionated embryos were disrupted in 2 ml of membrane lysis buffer (50 mM Tris, pH 7.5, 150 mM KCl, 5 mM $MgCl_2$, 0.25 M sucrose, 0.1 mM DTT, 1 mM PMSF) with 5 strokes of PestleA and 10 strokes of PestleB in a Dounce homogenizer (Kimble Kontes). The extract was centrifuged at 1000 × *g* for 10 min to pellet down cell debris and nuclei. The supernatant was mixed with 15.2 ml of 2.5 M sucrose and transferred to an SW27 tube. This mix was overlaid with 12.5 ml of 2.0 M sucrose followed with 7 ml of 0.5 M sucrose. Centrifugation was performed at 100,000 × *g* for 4 h. The membrane fraction at the interface of the 0.5 and 2.0 M sucrose layer was removed with a Pasteur pipette, mixed with 2 volumes of membrane lysis buffer, and centrifuged at 30,000 × *g* for 30 min (17).

Immunoprecipitation of Mega from Membrane Extracts—The membrane extracts were resuspended in 0.5 ml Nonidet P-40-lysis buffer (150 mM NaCl, 50 mM Tris, pH 8, 1 or 0.5% Nonidet P-40) to solubilize proteins from lipid bilayers. After incubation on ice for 30 min, the suspension was centrifuged at 30,000 × *g* (4 °C) for 30 min. For immunoprecipitation we used the Dynabeads® co-immunoprecipitation kit (Invitrogen) according to the manufacturer's protocol. The precipitated proteins were either analyzed by SDS-PAGE and Western blot or by mass spectrometry.

Mass Spectrometry—Proteins enriched by immune-precipitation were separated by one-dimensional PAGE (4–12% NuPAGE®, Invitrogen) and stained with colloidal Coomassie. Entire lanes were cut out into 23 slices and subjected to in-gel digestion with trypsin (18). Tryptic peptides were analyzed by LC-coupled-MSMS on an Orbitrap XL mass spectrometer (Thermo Fisher Scientific) under standard conditions. Fragment spectra were searched against the NCBI protein database (NCBI 20071008 with 54,234 *Drosophila* entries) with Mascot (Matrix Science) as the search engine. The following search parameters were used: carbamidomethylcysteine and oxidation of methionine as variable modifications, 2 miss cleavages allowed, precursor mass deviation was set to 5 ppm, fragment mass deviation to 0.5 Da, protein false positive rate was set to maximum 0.1%. Data were annotated using Scaffold (Proteome Software, Version 3.4.3) using the following parameters: minimum peptide and protein identification probability 80%, minimum 2 identified peptides per protein. Proteins identified in both immunoprecipitations (IPs) and control samples were quantified using spectral counting and Top3 TIC (total ion current of the top 3 peptides for each protein) methods within Scaffold. The non-normalized-fold change ratios with 95% significance for each IP are highlighted in *green* in supplemental Table 1. Detailed information about each protein (identified peptides, identification probability, mascot score, modifications) is provided in supplemental Table 2.

Immunochemistry—Whole-mount immunostainings of fixed embryos were performed as described previously (19). Primary antibodies used were the following. Mouse monoclonal anti-Mega antibody (anti-Mega mABs) directed against the peptide GYQPPRHHHSQSRSL (amino acids 238–252) was generated by GenScript (Piscataway, NJ). Rabbit anti-Crim antibodies directed against the peptides VTERRGARETITRDC (amino acids 61–75) and HTIKEHDVRRDYYTDT (amino acids 108–123) of Crim (*CG6038*) were generated by PSL GmbH (Heidelberg, Germany). Monoclonal antibody 2A12 (Developmental Studies Hybridoma Bank (DSHB), University of Iowa, Iowa City, IA) was used to visualize tracheal lumen. The rat anti-clathrin heavy chain (Chc) antibody was used in a 1:40 dilution for immunofluorescence labeling studies in whole mount embryos (20). Alexa633-conjugated wheat germ agglutinin (1:200, Molecular probes, Invitrogen) was used to label plasma membrane surfaces. Embryo fixation, fluorescence immunostainings, and confocal microscopy were performed as described (20). Each fluorochrome was scanned individually in single optical sections by using standard settings (LSM710, Zeiss Zen software) and a 63× LCI Plan Neofluar objective. Secondary antibodies used were the following: biotinylated goat anti-mouse immunoglobulin M (Jackson ImmunoResearch Laboratories, West Grove, PA); biotinylated horse anti-mouse immunoglobulin G (IgG) and biotinylated goat anti-rabbit IgG (Vector Laboratories, Burlingame, CA); goat anti-mouse IgG-Alexa568, goat anti-rabbit IgG-Alexa568, goat anti-mouse IgG-Alexa488, and goat anti-rabbit IgGAlexa488 (Invitrogen). Vectastain ABC elite kit (Vector Laboratories) and/or Tyramide Signal Amplification (PerkinElmer Life Sciences) were used to enhance signals. Image acquisition was performed with a Leica TCS SP2 (Leica Microsystems GmbH, Mannheim, Germany) and a Zeiss LSM780 (Carl Zeiss MicroImaging GmbH, Jena, Germany) confocal microscope.

Fly Strains and Genetic Crosses—Ectopic RNAi expression in the embryonic tracheal system was performed by crossing the driver *btl-GAL4* (21) with UAS-RNAi reporter lines (VDRC;

Downloaded from www.jbc.org at Max Planck Inst.Biophysikalische Chemie,Otto Hahn Bibl,Pf.2841,37018 Goettingen, on December 5, 2012

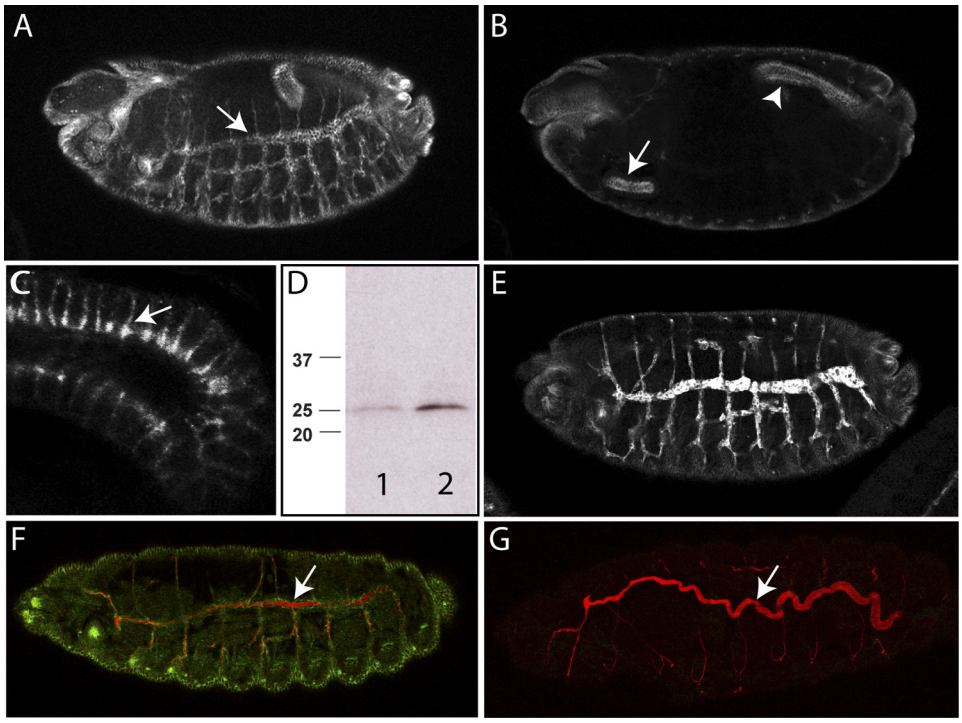

FIGURE 1. **The monoclonal anti-Mega AB 1H10F7 reveals high Mega specificity.** Whole-mount antibody staining of wild-type embryos at stage 15 (*A*–C) using the anti-Mega mAB 1H10F7 were visualized by confocal microscopy. *A* and *B* represent different focal planes of the same embryo. Mega is localized in the tracheal system (*arrow* in *A*), the salivary glands (*arrow* in *B*), and the hindgut (*arrowhead* in *B*). *C* shows a hindgut with the specific SJ staining of Mega. The anti-Mega mAB detects Mega specifically in the SJ of a hindgut epithelium (*arrow* in *C*). *D*, shown is an immunoblot of extracts from 0–20-h-old wild-type (*1*) and *btl-GAL4;UAS-mega* (*2*) embryos stained with the anti-Mega mAB. The mAB detects Mega specifically in extracts from wild-type (*1*) and *mega* overexpression (*2*) embryos. *E*, whole-mount antibody staining of *btl-GAL4;UAS-mega* embryos at stage 15 using the anti-Mega mAB is shown. Mega reveals massive accumulation in cells of the tracheal system. Shown is whole-mount staining of wild-type (*F*) and $mega^{G0012}$ mutant embryos (*G*) using the anti-Mega mAB (*green*) and chitin binding probe (*red*). Chitin-binding protein serves as marker for tracheal morphogenesis and reveals wild-type tracheal development (*arrow* in *F*) and the typical tortuous tracheal branches of *mega* mutant embryos (*arrow* in *G*). Although the anti-Mega mAB detects Mega in wild-type embryos (*green* in *F*) no Mega is detectable in *mega* mutant embryos (*G*).

Vienna *Drosophila* RNAi Center) at 25 °C. Balancers and marker chromosomes were obtained from the Bloomington Stock Center (Indiana University, Bloomington, IN).

RESULTS

Immunoprecipitation of Mega Protein Complexes—A prerequisite for the isolation of Mega protein complexes by immunoprecipitation is the availability of large quantities of highly specific antibodies. To obtain such antibodies, we produced monoclonal antibodies (mABs) directed against N-terminal cytoplasmic protein sequences of the SJ component Mega ("Experimental Procedures"). The anti-Mega mAB 1H10F7 detects the Mega protein specifically in the *Drosophila* embryo (Fig. 1, *A*–*C*) and on Western blots of embryonic protein extracts (Fig. 1*D*). In addition, the antibody detects high levels of *UAS/GAL4*-mediated (22) expression of Mega in embryos (Fig. 1*E*) and in embryonic extracts via Western blot analysis (Fig. 1*D*). Also, the anti-Mega mAB reveals the specific SJ localization of the claudin Mega (Fig. 1*C*). The anti-Mega mAB is very specific for Mega as it is able to detect Mega in wild-type embryos (Fig. 1*F*) but not in *mega* mutant embryos (Fig. 1*G*). Taken together, these results indicate that the anti-Mega mAB 1H10F7 is of high specificity and recognizes folded and denatured Mega, making it, therefore, suitable for immunoprecipitation experiments.

For the immunoprecipitations we used collections of 9–22-h-old *Drosophila* embryos, encompassing the developmental time in which SJs are formed and established (4). The embryos were used to prepare protein membrane extracts as described (see "Experimental Procedures"). Integral membrane proteins were solubilized from pellets of the membrane fractions by incubation with 0.5 or 1% Nonidet P-40 lysis buffer. The protein complexes were immunoprecipitated from the solubilization buffers using anti-Mega mAB 1H10F7 coupled to Dynabeads® and analyzed by SDS-PAGE and Western blot analysis (Fig. 2; "Experimental Procedures"). Mega was detectable in the solubilized fractions (Fig. 2, *B* and *D*) and after immunoprecipitation with anti-Mega mABs in the solubilized 1% Nonidet P-40 fraction (Fig. 2*B*). Mega was not detectable in the control immunoprecipitations using only Dynabeads® (Fig. 2, *B* and *D*) and after immunoprecipitation with anti-Mega mABs from the solubilized 0.5% Nonidet P-40 fraction (Fig. 2*D*). Although the immunoprecipitation of the 0.5% Nonidet P-40 fraction lacks detectable Mega by Western blot analysis (Fig. 2*D*) the subsequent mass spectrometry identified various proteins including Mega in this sample.

Mass Spectrometry of the Mega Protein Complex—The immunoprecipitates with anti-Mega mABs from the solubilized 0.5 and 1% Nonidet P-40 fractions as well as the corresponding controls *i.e.* immunoprecipitates with beads without coupled antibodies (see Fig. 2) were analyzed by mass spectrometry after in-gel digestion of entire PAGE lanes ("Experimental Procedures"). We identified 142 different proteins that

Downloaded from www.jbc.org at Max Planck Inst.Biophysikalische Chemie,Otto Hahn Bibl,Pf.2841,37018 Goettingen, on December 5, 2012

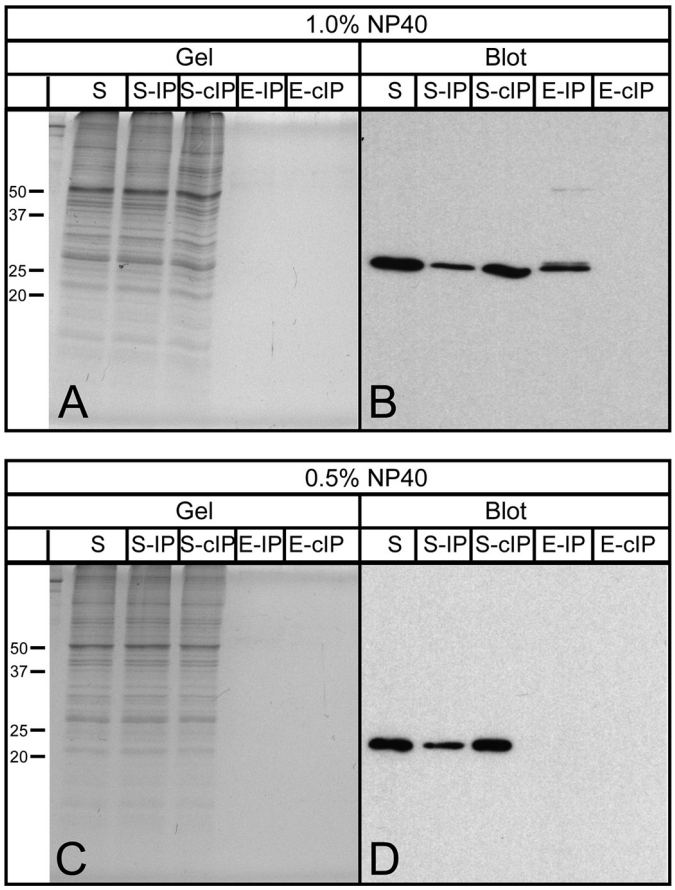

FIGURE 2. **Immunoprecipitation of the Mega protein complex using the anti-Mega mAB 1H10F7.** Protein membrane extracts of 9–22-h-old wild-type embryos were prepared, and IPs were performed with the anti-Mega mAB 1H10F7 as described ("Experimental Procedures"). The membrane fractions were solubilized by 1.0% Nonidet P-40 (*A* and *B*) or 0.5% Nonidet P-40 (*C* and *D*) in lysis buffer, aliquots were analyzed by SDS-PAGE (*A* and *C*) and immunoblots were probed with the anti-Mega mAB (*B* and *D*). The solubilized supernatants (*S*), the supernatants after IP (*S-IP*), the supernatants after control IP (*S-cIP*), the eluates after IP (*E-IP*), and the eluates after control IP (*E-cIP*) are shown. The *numbers* indicate the molecular mass in kilodaltons. E-IP from membrane fractions solubilized by 1.0% Nonidet P-40 lysis buffer contain detectable Mega protein (*B*), whereas membrane fractions solubilized by 0.5% Nonidet P-40 lysis buffer lack detectable Mega protein (*D*).

were present in both 0.5 and 1% Nonidet P-40 immunoprecipitates with anti-Mega mABs but not in the corresponding controls (supplemental Table 1). Thus, the SJ component Mega may interact with 142 different proteins. 10 of such proteins are *bona fide* SJ components, and the remaining 132 proteins may represent SJ or SJ-associated proteins (summarized in Table 1). To analyze their putative role for SJ formation, we performed an *in vivo* analysis by tissue-specific RNA interference (RNAi) gene knockdown experiments.

Functional Analysis of the Putative SJ Proteins—SJ protein complexes are essential for normal development and epithelial tissue integrity of tubular organs. We have used the *Drosophila* tracheal system as a read out system to study abnormal morphogenesis mediated by SJs defects. During embryogenesis the tracheal system forms specialized branches that fuse with adjacent branches, and consequently a three-dimensional tubular network is generated (23). During branch maturation, tracheal cells secrete chitin that forms a transient cylindrical matrix into the lumen of the tubes. The correct deposition of chitin in the apical extracellular matrix and its dynamic modification is necessary for the controlled dilation of the tubular walls (24–26). It is assumed that distinct classes of cargo vesicles facilitate apical trafficking of luminal components whereby one class depends on SJs to mediate normal transport and apical secretion of chitin deacetylases (27). During all stages of embryonic tracheal development the system is filled with liquid. This becomes replaced by gas in a process referred to as liquid clearance (LC) at the end of embryogenesis. The LC of the tubes creates a functional organ system that supplies oxygen to the tissues throughout larval stages (28, 29). The elaborate morphogenesis of the *Drosophila* tracheal system (Fig. 3, *A* and *B*) and LC of the tubes (Fig. 3*C*) critically depends on functional SJs. Mutations in genes that encode SJ components reveal elongated and tortuous tracheal branches during embryogenesis. Such mutants do not perform tracheal LC, probably due to disruption of the transepithelial barrier function (9–11). Hence, as expected, the tracheal-specific knockdown of *mega* gene expression by RNAi reveals tortuous tracheal branches (Fig. 3, *D* and *E*), failure to perform tracheal LC (Fig. 3*F*), and consequently lethality during the first instar larval stage (not shown).

To obtain information about the possible functions of Mega interacting proteins, we first analyzed whether these components are essential for normal tracheal development. For this we performed tissue-specific RNAi-mediated gene knockdown experiments using the *UAS/GAL4* system (22). The well established driver *btl-GAL4* was used to mediate RNAi expression ubiquitously in the developing tracheal system from stage 11 onward (see "Experimental Procedures"). The RNAi-mediated knockdowns of 74 genes in the developing tracheal system do not impair normal development and generate viable and fertile flies (Table 1), suggesting that these genes may not be essential for development and/or maintenance of tracheal branches during embryogenesis. Consequently, these genes may not play crucial roles for SJ formation. Thus, they were not further analyzed *in vivo*, although we cannot rule out essential functions of these genes due to inefficiency of RNAi-mediated gene knockdown. In contrast, the tracheal knockdowns of 55 genes cause lethality (Table 1), suggesting that these proteins are essential for normal trachea formation and/or function. We should point out that the *btl-GAL4* driver is not restricted to tracheal cells but is also expressed in midline glia and neuronal cells of the central nervous system. To examine whether the lethality is caused by affected tracheal SJs, we analyzed the phenotypes after RNAi-mediated gene knockdown using three different approaches. 1) We determined the developmental stage during which the animals die. 2) We analyzed the tracheal morphology during late embryogenesis using a specific tracheal marker. 3) We analyzed the tracheal LC process during the first instar larval stage. The results are summarized in Table 1. The progeny of 40 lines die during larval and/or pupal stages after RNAi-mediated gene knockdown with no discernable effects on tracheal development or LC (Fig. 3, *A–C*; not shown). Such animals develop a wild-type-like tracheal morphology (Fig. 3, *A* and *B*; not shown) and perform normal LC of the tracheal system during embryogenesis (Fig. 3*C*; not shown). Thus, the results suggest that this group of genes mediates essential functions during late larval or pupal stages but has no crucial func-

Downloaded from www.jbc.org at Max Planck Inst.Biophysikalische Chemie,Otto Hahn Bibl,Pf.2841,37018 Goettingen, on December 5, 2012

TABLE 1

***In vivo* analysis of the Mega interacting proteins**

The Mega interacting proteins were analysed by tissue-specific knockdown experiments of the corresponding genes (column 1, computational gene (GC) number: column 2, annotated proteins are indicated according to FlyBase (43)). For this the *UAS-RNAi* fly lines (column 3, transformant ID from the VDRC Stock Center) were crossed with the tracheal driver line *btl-GAL4,* and the progeny were analysed according to their survivability. Viable progeny (V) and progeny lethal during embryogenesis (E), larval stages (L1, L2, L3) and/or pupa (P) are indicated in column 4 (lethal stage). The tracheal morphology of lethal progeny were analysed by 2A12 antibody staining, and the LC of first instar larvae was analysed by brightfield light microscopy (for details, see Fig. 3). Published SJ components are indicated. Abbreviations: V, viable; n.a., not available; n.d., not done; net.def., tracheal network defects.

CG number	btl-Gal4 X RNAi viable		CG number			btl-Gal4 X RNAi		
	annotated proteins	transformant ID		annotated proteins	transformant ID	lethal stage	tracheal morphology	liquid clearance (LC)
1548	CathD	31012	1821	Ribosomal protein L31	104467	L1	WT-like	normal LC
1599		13317	2107		n.a.			
1665		106465	2139	Aralar1	n.a.			
1751	Spase 25-subunit	51149	2286	NADH:ubiquinone reductase 75kD subunit precursor	100733	P	WT-like	normal LC
2093	Vacuolar protein sorting13	29971	2358	Twisted bristles roughened eye	9055	L1	WT-like	normal LC
2204	G protein oa 47A	19124	2746	Ribosomal protein L19	108309	L1	WT-like	normal LC
2791	CD98 heavy chain	108365	3539	SLY-1 homologous	105669	L2	WT-like	normal LC
3024	Torp4a	110073	3902		n.a.			
3039	Optic ganglion reduced	103816	3921		52608	L1-L2	mega-like	no LC
3161	Vacuolar H+ ATPase subunit 16 1	49291	3921		107348	L1	mega-like	no LC
3321		46764	3922	Ribosomal protein S17	n.a.			
3424	Pathetic	100519	4046	Ribosomal protein S16	100610	L1-L2	WT-like	normal LC
3446		42697	4169		100818	L3-P	WT-like	normal LC
3566		102685	4679		38111	L3-P	WT-like	normal LC
3683		25961	4918	Ribosomal protein LP2	100684	L1-L2	WT-like	normal LC
3887		105430	5012	Mitochondrial ribosomal protein L12	100496	L3-P	WT-like	normal LC
4389		100021	5520	Glycoprotein 93	n.a.			
4581	Thiolase	105500	5916		110561	n.d.	n.d.	n.d.
5289	Proteasome 26S subunit subunit 4 ATPase	105973	6025	Arflike at 72A	106474	L3-P	WT-like	normal LC
5554		20101	6030	ATP synthase, subunit d	104353	P	WT-like	normal LC
5676		100557	6038	Crimpled	30379	L1	mega-like	no LC
5804		100642	6105	Lethal (2) 06225	107311	L3-P	WT-like	normal LC
5885		105974	6343	NADH:ubiquinone reductase 42kD subunit precursor	14444	P	WT-like	normal LC
6453		106254	6370		107068	L1-L2	WT-like	normal LC
6588	Fasciclin 1	101779	6455		106757	P	WT-like	normal LC
6666	Succinate dehydrogenase C	6031	6512		8515	P	WT-like	normal LC
6782	Scheggia	50714	6815	Belphegor	110208	L3-P	WT-like	normal LC
7111	Receptor of activated protein kinase C1	104470	6851	Mitochondrial carrier homolog 1	44306	P	WT-like	normal LC
7144	Lysine ketoglutarate reductase	51346	7014	Ribosomal protein S5b	27792	L2	WT-like	normal LC
7263	Apoptosis inducing factor	2544	7394		9210	E	net.def.	no LC
7461		28029	7434	Ribosomal protein L22	104506	L1	WT-like	normal LC
7563	Calpain	101294	7603		100911	L2-P	WT-like	normal LC
7610	ATP synthase-gamma chain	16539	7726	Ribosomal protein DL11	101731	L1	net.def.	no LC
7830		4253	8210	vacuolar ATPase subunit A	110160	P	WT-like	normal LC
7870		2802	8280	Elongation factor 1alpha48D	104502	E-L1	net.def.	no LC
8075	Strabismus	100819	8385	ADP ribosylation factor 79F	103572	L1-L2	WT-like	normal LC
8507		104321	8416	Rho1	12734	L1-L2	net.def.	no LC
8583	Sec63	33281	8707	dRagC	107203	P	WT-like	normal LC
8937	Heat shock protein cognate 1	45596	9012	Clathrin heavy chain	103383	L1	mega-like	partial LC
9000	Prenyl protease type I	105431	9172		23256	P	WT-like	normal LC
9066	Membrane steroid binding protein	45182	10130	Sec61beta	8785	L1	WT-like	no LC
9231		105726	10423	Ribosomal protein S27	107108	L1-L2	net.def.	no LC
9380		4070	10545	G protein beta-subunit 13F	31257	P	WT-like	normal LC
9416		106330	10545		100011	P	WT-like	normal LC
9539	Sec61alpha	42763	10652	Ribosomal protein L30	101391	L1	WT-like	normal LC
9541		102912	11015		30892	L1	net.def.	no LC
10067	Actin 57B	102129	11098	Transport and Golgi organization 1	21594	L1-P	WT-like	normal LC
10326		104790	11271	Ribosomal protein S12	109381	L1-L2	WT-like	normal LC
10373	Jwa ortholog	6375	12079		103412	P	WT-like	normal LC
10803		106599	12400		37463	P	WT-like	normal LC
11064	Retinoid- and fatty acid-binding glycoprotein	100944	12740	Ribosomal protein L28	104021	L1-L2	WT-like	normal LC
11081	plexin A	4740	13240	lethal (2) 35Di	110295	L3-P	WT-like	normal LC
11129	Yolk protein 3	46787	15693	Ribosomal protein S20	105298	L2	WT-like	normal LC
11137		108256	18001	Ribosomal protein L38	23565	E-L1	net.def.	no LC
11200	Carbonyl reductase	4725	18076	Short stop	n.a.			
11567	Cytochrome P450 reductase	46715	30415		106403	L3-P	WT-like	normal LC
11739		44562	31195		104743	L3-P	WT-like	normal LC
11785	Baiser	100612	31605	Basigin	43306	P	WT-like	normal LC
11958	Calnexin 99A	100740	33303		107778	L2	WT-like	normal LC
12203		101489						
12891	Withered	105400						
14103		8428						
14214	Sec61gamma	100603						
15092		104543						
15113	Serotonin receptor 1B	9558						
17246	Succinate dehydrogenase A	110440						
17320	Sterol carrier protein X-related thiolase	106851						
17759	G protein alpha49B	105300						
18347		106319						
30404	Transport and Golgi organization 11	29385						
32230		101482						
32775	GlcAT-I	107840						
33129		107365						

CG number	published SJ components	reference
1084	Contactin	[44]
1634	Neuroglian	[45]
3665	Fasciclin 2	[46]
5670	Na+, K+ ATPase alpha-subunit	[47]
5803	Fasciclin 3	[48]
6827	Neurexin IV	[49]
8663	Nervana 3	[50]
10620	Melanotransferrin	[16]
12369	Lachesin	[51]
14779	Megatrachea	[9]

Downloaded from www.jbc.org at Max Planck Inst.Biophysikalische Chemie,Otto Hahn Bibl,Pf.2841,37018 Goettingen, on December 5, 2012

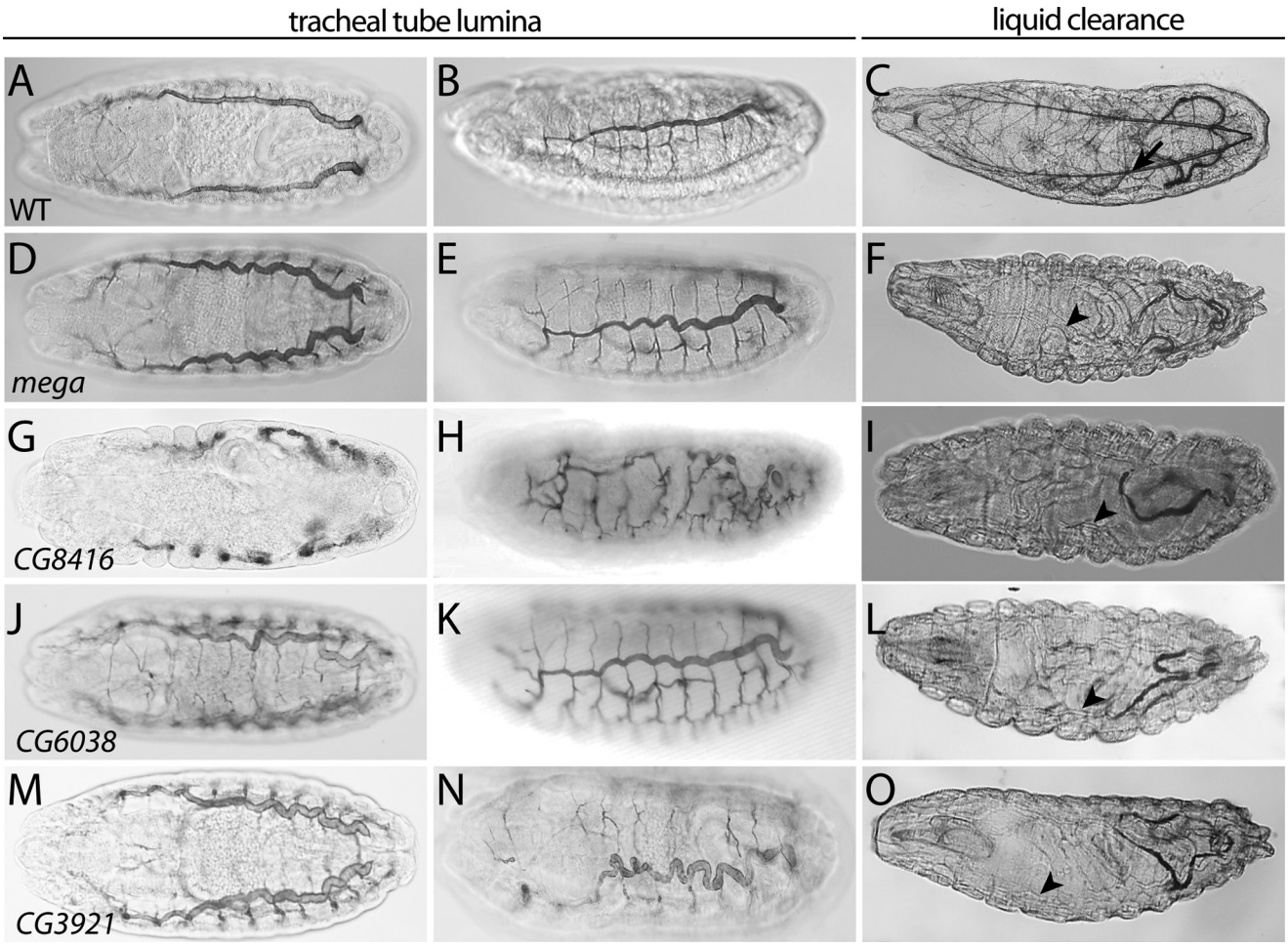

FIGURE 3. **RNAi-mediated tracheal phenotypes.** Whole-mount antibody staining of wild-type (*A* and *B*), *btl-GAL4* driven *UAS-RNAi-50306-mega* (*D* and *E*), *UAS-RNAi-12734* (*CG8416*; *G* and *H*), *UAS-RNAi-30379* (*CG6038*; *J* and *K*), and *UAS-RNAi-52608* (*CG3921*; *M* and *N*) embryos stained with the tracheal luminal marker 2A12 is shown. Brightfield light microscopic pictures of wild-type (*C*), *btl-GAL4* driven *UAS-RNAi-50306-mega* (*F*), *UAS-RNAi-12734* (*I*), *UAS-RNAi-30379* (*L*), and *UAS-RNAi-52608* (*O*) first instar larvae. The tracheal expression of *RNAi-50306-mega* reveals *mega*-like tortuous and elongated tracheal branches (*D* and *E*) similar as found for *mega* mutant embryos (9). The tracheal expression of *RNAi-12734* reveals tracheal network defects (*G* and *H*), the expression of *RNAi-30379* generates *mega*-like tracheal phenotypes (*J* and *K*), and *RNAi-52608* expression mediates strong *mega*-like tortuous tracheal branches (*M* and *N*). Wild-type first instar larvae show normal tracheal liquid clearance (*arrow* in *C*), whereas expression of *RNAi-50306-mega* (*F*) *RNAi-12734* (*I*), *RNAi-30379* (*L*), and *RNAi-52608* (*O*) reveal a lack of liquid clearance in first instar larvae (*arrowheads* in *F*, *I*, *L*, *O*). *A*, *D*, *G*, *J*, and *M* are dorsal, and *B*, *E*, *H*, *K*, and *N* are lateral views of embryos.

tion during early tracheal development. RNAi-mediated tracheal knockdown of seven genes leads to the disruption of the tracheal network (Fig. 3, *G* and *H*; not shown), loss of tracheal LC (Fig. 3*I*; not shown) and consequently death during embryogenesis or first instar larval stage. The tracheal networks are disrupted at varied positions in different embryos suggesting that no specific cell types, *e.g.* fusion cells of the tracheal system are affected by these RNAi knockdowns. Rather, the results suggest that general cell functions are influenced, leading to the disruption of cell-cell interconnections.

The most interesting group of genes is characterized by RNAi-mediated phenotypes resembling SJ mutant phenotypes, *i.e.* tortuous tracheal branches, similar to what is observed for *mega* mutant embryos. This group consists of the *clathrin heavy chain* gene (*chc*; *CG9012*) (30, 31), the recently identified gene *crimpled* (*crim*; *CG6038*) (15), and the uncharacterized gene *CG3921,* which encodes a putative member of the scavenger receptor protein family (supplemental Fig. 1; see "Discussion"). The RNAi-mediated tracheal phenotypes of *chc* (not shown) and *crim* (Fig. 3, *J* and *K*) are similar and comparable to the RNAi-mediated *mega* phenotype (Fig. 3, *D* and *E*). In contrast, tracheal knockdown of *CG3921* reveals an even stronger phenotype, *i.e.* the tracheal system shows more enhanced tortuous branches (Fig. 3, *M* and *N*) than found in the RNAi-mediated *mega* phenotype (Fig. 3, *D* and *E*). In addition, all three members of this group reveal RNAi-mediated knockdown larvae that lack normal tracheal LC (see Fig. 3*F* for *mega*, Fig. 3*L* for *crim*, and Fig. 3*O* for *CG3921*).

Chc components assemble with numerous adaptor proteins to establish clathrin-coated vesicles, which mediate cargo selective endocytosis (31). In the *Drosophila* tracheal system, it was demonstrated that Chc is required for tube length control and LC of the tracheal tubes (28, 29), consistent with our RNAi-mediated *chc* knockdown results (Table 1). The subcellular Chc localization appears dynamic in *Drosophila* and is associated with early endocytotic vesicles at or close to the plasma membrane (20). Our binding studies suggest that Mega associates with the Chc complex (Table 1). Thus, we performed co-immunofluorescence stainings in late wild-type embryos and found partial co-localization of Mega and Chc (Fig. 4, *B–E*). In addi-

Downloaded from www.jbc.org at Max Planck Inst.Biophysikalische Chemie,Otto Hahn Bibl,Pf.2841,37018 Goettingen, on December 5, 2012

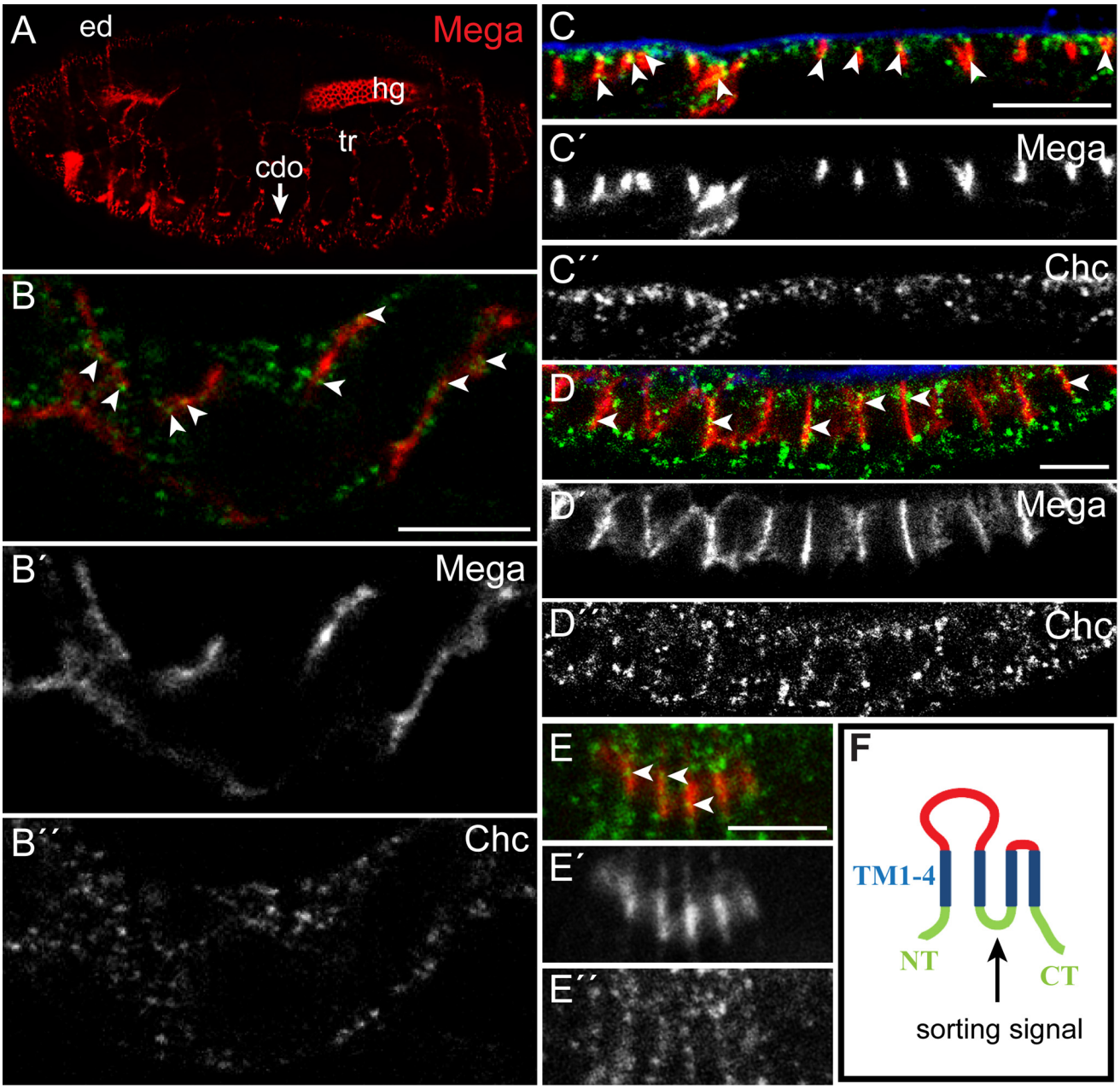

FIGURE 4. **Mega co-localizes with Chc at the membrane.** *A–E*, shown is whole-mount antibody double staining of stage 17 wild-type embryos with anti-Mega mAB and anti-Chc AB. *A*, the confocal image shows Mega (*red*) localization in trachea (*tr*), hindgut (*hg*), epidermis (*ed*), and chordotonal organs (*cdo*; *arrow*). Merged images of Mega (*red*) and Chc (*green*) are shown in the trachea (*B*), the epidermis (*C*), the hindgut (*D*), and the chordotonal organ (*E*). The corresponding images of Mega (*B′–E′*) and Chc (*B″–E″*) are shown in *gray*. Wheat germ agglutinin marks the apical cell membrane surface (*blue* in *C* and *D*). The *arrowheads* indicate Chc-positive vesicles partially co-localizing with Mega. *F*, shown is a scheme of the predicted Mega protein structure; transmembrane domains are indicated in *blue*, intracellular regions are in *green*, and extracellular regions are in *red*. A putative sorting signal (YXXφ sequence; φ is a bulky hydrophobic residue, and *X* is any amino acid) (32) that mediates targeting into clathrin-coated vesicles is localized in the intracellular loop (*arrow*; residue 146–149; YEWL) of Mega. CT, C terminus; *NT*, N terminus. *Scale bars* represent 5 μm.

tion, *in silico* analysis revealed a sorting sequence motif in Mega (Fig. 4*F*) associated with clathrin-mediated endocytosis of transmembrane proteins (32). These results indicate a close contact of Mega with Chc and Mega endocytosis via clathrin-coated vesicles.

It has recently been shown that the Mega interaction partner Crim is involved in SJ formation. However, the intracellular localization of Crim was yet unknown. Thus, we generated an anti-Crim antibody ("Experimental Procedures") and analyzed the intracellular Crim distribution (Fig. 5). Crim co-localizes with the SJ marker Mega in apical membrane regions of tracheal (Fig. 5*A*), hindgut (Fig. 5*B*), and salivary gland cells (Fig. 5*C*). Thus, our results indicate that Crim represents a *bona fide* SJ protein and suggest that Crim acts as a binding partner of Mega within the SJ.

DISCUSSION

This paper presents the first comprehensive proteomic study of an invertebrate claudin protein complex. We used the highly specific anti-Mega monoclonal antibody for immunoprecipita-

Downloaded from www.jbc.org at Max Planck Inst.Biophysikalische Chemie,Otto Hahn Bibl,Pf.2841,37018 Goettingen, on December 5, 2012

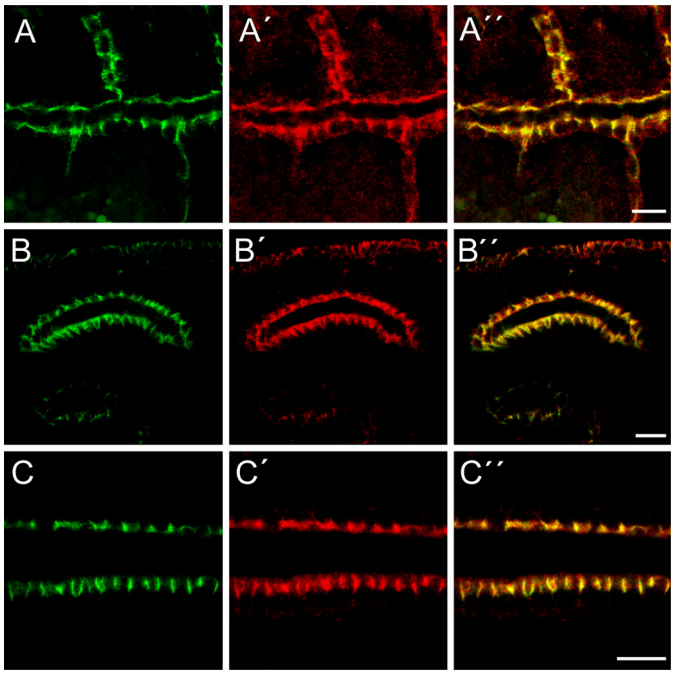

FIGURE 5. **Crim represents a *bona fide* SJ component.** Whole-mount antibody double staining of stage 17 wild-type embryos with anti-Mega mAB and anti-Crim AB (see "Experimental Procedures"). Merged images of Mega (*green*, *A–C*) and Crim (*red*, *A′–C′*) reveal co-localization of the proteins (*yellow*, *A″–C″*) in the tracheal system (*A″*), the salivary gland (*B″*), and the hindgut (*C″*). Co-localization with the SJ marker Mega (9) shows that Crim localization is confined to SJs during embryogenesis. *Scale bars* represent 10 μm.

tion of membrane proteins via their interaction with the *Drosophila* claudin Mega. Although the membrane proteins were solubilized from the lipid bilayer by two different concentrations of detergent (1% and 0.5% Nonidet P-40), the sets of Mega-interacting proteins are very similar after immunoprecipitation followed by mass spectrometry. However, under the less stringent 0.5% Nonidet P-40 conditions, a lower total protein amount was immunoprecipitated. This led to the detection of Mega via the very sensitive mass spectrometry analysis but not via Western blot analysis.

Our immune-precipitation studies revealed a set of 142 proteins that potentially interact with the claudin Mega. These proteins include 10 *bona fide* SJ components that represent most of the SJ components identified so far and, thus, serve as proof of concept for our analysis. In contrast, the high number of established and putative ribosomal proteins identified after immunoprecipitation suggests unspecific binding of these highly abundant proteins. However, we cannot exclude specific binding of one or more of such factors to the SJ protein complex. Therefore, to avoid biased results, we performed an *in vivo* analysis of the entire repertoire of the 142 proteins identified by mass spectrometry.

We show that the RNAi-mediated tracheal knockdown of the Mega interaction partner Rho1 reveal tracheal network disruptions and a lack of tracheal branch interconnection. It has previously been shown that the RhoGTPase Rho1 acts as a substrate of the RhoGAP enzyme Crossveinless-c (Cv-c) that affects actin-myosin apical distribution, likely by regulation of Rho1 activity (33). Embryos mutant for *cv-c* or *rho1* reveal affected tracheal cell invagination, which generates tracheal phenotypes similar to the RNAi-mediated Rho1 knockdown phenotypes. During the later stages of development Rho1 regulates adherence junctions during morphogenesis (34). However, additional Rho1 accumulation in the region of SJs (34) and our finding of the potential Mega-Rho1 interaction may also suggest regulation of SJs via Rho1 binding to the claudin Mega.

It has been proposed that endocytosis is involved in the recycling of the SJ component Melanotransferrin to the apicolateral membrane region where it forms complexes with Neurexin IV, Contactin, and Neuroglian (16). Importantly, our data provide evidence that Mega participates in this multiprotein complex formation as all four proteins co-precipitate with Mega. We further found that the previously characterized protein clathrin heavy chain (Chc) interacts with Mega, and our *in vivo* analysis revealed that Chc is essential for normal tracheal morphogenesis and gas filling of the tubes. Previous investigations identified caveolin- and clathrin-mediated forms of endocytosis important for TJ components in vertebrates (35, 36). For example, studies in human alveolar and T84 intestinal cells demonstrate Claudin internalization via clathrin vesicles (37, 38). In *Drosophila*, molecular mechanisms of claudin endocytosis are poorly understood. Caveolin has not been identified in the fly, whereas Chc, the main component of clathrin-mediated endocytosis, is expressed in a vesicle-like pattern within the cytoplasm and at the plasma membrane (20). Interestingly, the Mega sequence contains a conserved sorting signal for clathrin-mediated endocytosis similar to that described in the human Claudin 4 sequence (37). This motif is usually situated within cytosolic protein domains (32). Consistently, the Mega sorting motif is localized within the intracellular loop framed by the second and third transmembrane domains. However, the short distance between the sorting signal in Mega and the transmembrane domain is unusual for such motifs (32). Based on the co-localization of Mega and Chc and the conserved sorting signal, we suggest similar clathrin-dependent mechanisms of *Drosophila* and vertebrate claudin endocytosis and turnover at the plasma membrane. Thus, Mega internalization may play a crucial role in the remodeling of SJs, as it has been observed for TJ remodeling by claudins in vertebrates (39).

Our immunoprecipitation experiments indicate an association of Mega with all three subunits, Sec61α, Sec61β, and Sec61γ, of the Sec61p complex. Oligomers of the Sec61p complex make up the protein translocation channel at the endoplasmic reticulum. Protein translocation across the endoplasmic reticulum is the initial step in the biogenesis of secretory and membrane proteins (40). Because intact SJs are essential for the secretion of the chitin deacetylases Serpentine and Vermiform (27, 41), we suggest that these particular secretion processes depend on an interaction of the SJ component Mega with the Sec61p complex proteins Sec61α, Sec61β, and Sec61γ. We cannot exclude the possibility that Mega and Sec61p complex protein interaction occurs during the transport of Mega across the protein translocation channel. However, we favor the model of an interaction between the Sec61p complex and SJs via the SJ component Mega because it integrates the essential requirements of Mega for SJ formation and the secretion of Serpentine and Vermiform via the Sec61p complex as well.

Downloaded from www.jbc.org at Max Planck Inst.Biophysikalische Chemie,Otto Hahn Bibl,Pf.2841,37018 Goettingen, on December 5, 2012

The Mega binding partner Crim is a member of the Ly6 protein family, whose members are characterized by glycosyl phosphatidylinositol-anchored, cysteine-rich cell surface molecules. It has recently been shown that at least four members of this group, Boudin (42), Crim, Crooked, and Coiled (15), are required for SJ formation. However, in contrast to Crooked and Coiled, which are required for SJ formation and localized in SJs (15), it was shown that Boudin requirements for SJ organization are non-cell-autonomous, and Boudin is secreted extracellularly (42). Thus it was of particular interest to analyze the intracellular distribution of Crim. Our finding that Crim co-localizes with the SJ marker Mega in all analyzed tissues indicate that Crim represents a *bona fide* SJ component as shown for the Ly6 family members Crooked and Coiled. Thus, we speculate that Mega, Crim, and other Ly6 proteins participate in the formation of multiprotein complexes to mediate their functional SJ association.

The immune-precipitation experiments show that Mega interacts with an uncharacterized protein encoded by *CG3921*. The RNAi-mediated tracheal knockdown of *CG3921* revealed tracheal phenotypes during embryogenesis that are reminiscent of SJ mutant phenotypes. Furthermore, *CG3921* tracheal knockdown embryos fail to perform gas filling of the tracheal branches as found in embryos with affected SJs. *CG3921* encodes a conserved 3115-amino acid long putative scavenger receptor protein (supplemental Fig. 1 and 2) (43). Thus, we assume that *CG3921* protein participates in the SJ protein complex at the lateral plasma membrane. Future experiments including mutant analysis and localization studies of CG3921 protein by specific antibodies will determine whether this putative scavenger receptor participates in SJ function and tracheal morphogenesis.

Acknowledgments—We thank the Vienna Drosophila RNAi Center and the Bloomington Drosophila stock center for scientific material. We are grateful to U. Löhr, R. Pflanz, U. Schäfer, and members of the department "Molekulare Entwicklungsbiologie" for comments on the manuscript and for discussions. We thank M. Raabe for excellent help. Special thanks go to H. Jäckle for providing a stimulating environment.

REFERENCES

1. Farquhar, M. G., and Palade, G. E. (1963) Junctional complexes in various epithelia. *J. Cell Biol.* **17,** 375–412
2. Schneeberger, E. E., and Lynch, R. D. (1992) Structure, function, and regulation of cellular tight junctions. *Am. J. Physiol.* **262,** L647–L661
3. Madara, J. L. (1998) Regulation of the movement of solutes across tight junctions. *Annu. Rev. Physiol.* **60,** 143–159
4. Tepass, U., Tanentzapf, G., Ward, R., and Fehon, R. (2001) Epithelial cell polarity and cell junctions in *Drosophila*. *Annu. Rev. Genet.* **35,** 747–784
5. Knust, E., and Bossinger, O. (2002) Composition and formation of intercellular junctions in epithelial cells. *Science* **298,** 1955–1959
6. Turksen, K., and Troy, T. C. (2004) Barriers built on claudins. *J. Cell Sci.* **117,** 2435–2447
7. Furuse, M., and Tsukita, S. (2006) Claudins in occluding junctions of humans and flies. *Trends Cell Biol.* **16,** 181–188
8. Mineta, K., Yamamoto, Y., Yamazaki, Y., Tanaka, H., Tada, Y., Saito, K., Tamura, A., Igarashi, M., Endo, T., Takeuchi, K., and Tsukita, S. (2011) Predicted expansion of the claudin multigene family. *FEBS Lett.* **585,** 606–612
9. Behr, M., Riedel, D., and Schuh, R. (2003) The claudin-like megatrachea is essential in septate junctions for the epithelial barrier function in *Drosophila*. *Dev. Cell* **5,** 611–620
10. Wu, V. M., Schulte, J., Hirschi, A., Tepass, U., and Beitel, G. J. (2004) Sinuous is a *Drosophila* claudin required for septate junction organization and epithelial tube size control. *J. Cell Biol.* **164,** 313–323
11. Nelson, K. S., Furuse, M., and Beitel, G. J. (2010) The *Drosophila* claudin Kune-kune is required for septate junction organization and tracheal tube size control. *Genetics* **185,** 831–839
12. Hamazaki, Y., Itoh, M., Sasaki, H., Furuse, M., and Tsukita, S. (2002) Multi-PDZ domain protein 1 (MUPP1) is concentrated at tight junctions through its possible interaction with claudin-1 and junctional adhesion molecule. *J. Biol. Chem.* **277,** 455–461
13. Poliak, S., Matlis, S., Ullmer, C., Scherer, S. S., and Peles, E. (2002) Distinct claudins and associated PDZ proteins form different autotypic tight junctions in myelinating Schwann cells. *J. Cell Biol.* **159,** 361–372
14. Itoh, M., Furuse, M., Morita, K., Kubota, K., Saitou, M., and Tsukita, S. (1999) Direct binding of the three tight junction- associated MAGUKs, ZO-1, ZO-2, and ZO-3, with the COOH termini of claudins. *J. Cell Biol.* **147,** 1351–1363
15. Nilton, A., Oshima, K., Zare, F., Byri, S., Nannmark, U., Nyberg, K. G., Fehon, R. G., and Uv, A. E. (2010) Crooked, coiled, and crimpled are three Ly6-like proteins required for proper localization of septate junction components. *Development* **137,** 2427–2437
16. Tiklová, K., Senti K. A., Wang, S., Gräslund, A., and Samakovlis, C. (2010) Epithelial septate junction assembly relies on melanotransferrin iron binding and endocytosis in *Drosophila*. *Nat. Cell Biol.* **12,** 1071–1077
17. Zhang, C. X., and Hsieh, T-S. (2000) in *Drosophila Protocols* (Sullivan, W., Ashburner, M., Hawley, R. S., eds) pp. 563–570, Cold Spring Harbor Laboratory Press, Cold Spring Harbor, NY
18. Shevchenko, A., Wilm, M., Vorm, O., and Mann, M. (1996) Mass spectrometric sequencing of proteins silver-stained polyacrylamide gels. *Anal. Chem.* **68,** 850–858
19. Patel, N. H. (1994) Imaging neuronal subsets and other cell types in whole-mount *Drosophila* embryos and larvae using antibody probes. *Methods Cell Biol.* **44,** 445–487
20. Wingen, C., Stümpges, B., Hoch, M., and Behr, M. (2009) Expression and localization of clathrin heavy chain in *Drosophila* melanogaster. *Gene Expr. Patterns* **9,** 549–554
21. Shiga, Y., Tanaka-Matakatsu, M., and Hayashi, S. (1996) A nuclear GFP/β-galactosidase fusion protein as a marker for morphogenesis in living *Drosophila* tracheal system. *Dev. Growth Differ.* **38,** 99–106
22. Brand, A. H., and Perrimon, N. (1993) Targeted gene expression as a means of altering cell fates and generating dominant phenotypes. *Development* **118,** 401–415
23. Affolter, M., and Shilo, B. Z. (2000) Genetic control of branching morphogenesis during *Drosophila* tracheal development. *Curr. Opin. Cell Biol.* **12,** 731–735
24. Devine, W. P., Lubarsky, B., Shaw, K., Luschnig, S., Messina, L., and Krasnow, M. A. (2005) Requirement for chitin biosynthesis in epithelial tube morphogenesis. *Proc. Natl. Acad. Sci. U.S.A.* **102,** 17014–17019
25. Tonning, A., Hemphälä, J., Tång, E., Nannmark, U., Samakovlis, C., and Uv, A. (2005) A transient luminal chitinous matrix is required to model epithelial tube diameter in the *Drosophila* trachea. *Dev. Cell* **9,** 423–430
26. Petkau, G., Wingen, C., Jussen, L. C., Radtke, T., and Behr, M. (2012) Obstructor-a is required for epithelial extracellular matrix dynamics, exoskeleton function, and tubulogenesis. *J. Biol. Chem.* **287,** 21396–21405
27. Wang, S., Jayaram, S. A., Hemphälä, J., Senti, K. A., Tsarouhas, V., Jin, H., and Samakovlis, C. (2006) Septate junction-dependent luminal deposition of chitin deacetylases restricts tube elongation in the *Drosophila* trachea. *Curr. Biol.* **16,** 180–185
28. Behr, M., Wingen, C., Wolf, C., Schuh, R., and Hoch, M. (2007) Wurst is essential for airway clearance and respiratory-tube size control. *Nat. Cell Biol.* **9,** 847–853
29. Tsarouhas, V., Senti, K. A., Jayaram, S. A., Tiklová, K., Hemphälä, J., Adler, J., and Samakovlis, C. (2007) Sequential pulses of apical epithelial secretion and endocytosis drive airway maturation in *Drosophila*. *Dev. Cell* **13,** 214–225

Downloaded from www.jbc.org at Max Planck Inst.Biophysikalische Chemie,Otto Hahn Bibl,Pf.2841,37018 Goettingen, on December 5, 2012

30. Bazinet, C., Katzen, A. L., Morgan, M., Mahowald, A. P., and Lemmon, S. K. (1993) The *Drosophila* clathrin heavy chain gene. Clathrin function is essential in a multicellular organism. *Genetics* **134,** 1119–1134
31. Ungewickell, E. J., and Hinrichsen, L. (2007) Endocytosis. Clathrin-mediated membrane budding. *Curr. Opin. Cell Biol.* **19,** 417–425
32. Bonifacino, J. S., and Traub, L. M. (2003) Signals for sorting of transmembrane proteins to endosomes and lysosomes. *Annu. Rev. Biochem.* **72,** 395–447
33. Brodu, V., and Casanova, J. (2006) The RhoGAP *crossveinless-c* links *trachealess* and EGFR signaling to cell shape remodeling in *Drosophila* tracheal invagination. *Genes Dev.* **20,** 1817–1828
34. Fox, D. T., Homem, C. C., Myster, S. H., Wang, F., Bain, E. E., and Peifer, M. (2005) Rho1 regulates *Drosophila* adherens junctions independently of p120ctn. *Development* **132,** 4819–4831
35. Marchiando, A. M., Shen, L., Graham, W. V., Weber, C. R., Schwarz, B. T., Austin, J. R., 2nd, Raleigh, D. R., Guan, Y., Watson, A. J., Montrose, M. H., and Turner, J. R. (2010) Caveolin-1-dependent occludin endocytosis is required for TNF-induced tight junction regulation *in vivo*. *J. Cell Biol.* **189,** 111–126
36. Ivanov, A. I., Nusrat, A., and Parkos, C. A. (2004) Endocytosis of epithelial apical junctional proteins by a clathrin-mediated pathway into a unique storage compartment. *Mol. Biol. Cell* **15,** 176–188
37. Ivanov, A. I., Nusrat A., and Parkos, C. A. (2004) The epithelium in inflammatory bowel disease. Potential role of endocytosis of junctional proteins in barrier disruption. *Novartis Found. Symp.* **263,** 115–124; discussion 124–32, 211–8
38. Daugherty, B. L., Mateescu, M., Patel, A. S., Wade, K., Kimura, S., Gonzales, L. W., Guttentag, S., Ballard, P. L., and Koval, M. (2004) Developmental regulation of claudin localization by fetal alveolar epithelial cells. *Am. J. Physiol. Lung Cell. Mol. Physiol.* **287,** L1266–L1273
39. Matsuda, M., Kubo, A., Furuse, M., and Tsukita, S. (2004) A peculiar internalization of claudins, tight junction-specific adhesion molecules, during the intercellular movement of epithelial cells. *J. Cell Sci.* **117,** 1247–1257
40. Osborne, A. R., Rapoport, T. A., and van den Berg, B. (2005) Protein translocation by the Sec61/SecY channel. *Annu. Rev. Cell Dev. Biol.* **21,** 529–550
41. Luschnig, S., Bätz, T., Armbruster, K., and Krasnow, M. A. (2006) Serpentine and vermiform encode matrix proteins with chitin binding and deacetylation domains that limit tracheal tube length in *Drosophila*. *Curr. Biol.* **16,** 186–194
42. Hijazi, A., Masson, W., Augé, B., Waltzer, L., Haenlin, M., and Roch, F. (2009) *Boudin* is required for septate junction organization in *Drosophila* and codes for a diffusible protein of the Ly6 superfamily. *Development* **136,** 2199–2209
43. McQuilton, P., St Pierre, S. E., Thurmond, J., and FlyBase Consortium (2012) FlyBase 101. The basics of navigating FlyBase. *Nucleic Acids Res.* **40,** D706–D714
44. Faivre-Sarrailh, C., Banerjee, S., Li, J., Hortsch, M., Laval, M., and Bhat, M. A. (2004) *Drosophila* contactin, a homolog of vertebrate contactin, is required for septate junction organization and paracellular barrier function. *Development* **131,** 4931–4942
45. Genova, J. L., and Fehon, R. G. (2003) Neuroglian, gliotactin, and the Na^+/K^+ ATPase are essential for septate junction function in *Drosophila*. *J. Cell Biol.* **161,** 979–989
46. Hemphälä, J., Uv, A., Cantera, R., Bray, S., and Samakovlis, C. (2003) Grainy head controls apical membrane growth and tube elongation in response to Branchless/FGF signaling. *Development* **130,** 249–258
47. Paul, S. M, Ternet, M., Salvaterra, P. M., and Beitel, G. J. (2003) The Na^+/K^+ ATPase is required for septate junction function and epithelial tube-size control in the *Drosophila* tracheal system. *Development* **130,** 4963–4974
48. Snow, P. M., Bieber, A. J., and Goodman, C. S. (1989) Fasciclin III. A novel homophilic adhesion molecule in *Drosophila*. *Cell* **59,** 313–323
49. Banerjee, S., Pillai, A. M., Paik, R., Li, J., and Bhat, M. A. (2006) Axonal ensheathment and septate junction formation in the peripheral nervous system of *Drosophila*. *J. Neurosci.* **26,** 3319–3329
50. Paul, S. M., Palladino, M. J., and Beitel, G. J. (2007) A pump-independent function of the Na,K-ATPase is required for epithelial junction function and tracheal tube-size control. *Development* **134,** 147–155
51. Llimargas, M., Strigini, M., Katidou, M., Karagogeos, D., and Casanova, J. (2004) Lachesin is a component of a septate junction-based mechanism that controls tube size and epithelial integrity in the *Drosophila* tracheal system. *Development* **131,** 181–190

Downloaded from www.jbc.org at Max Planck Inst.Biophysikalische Chemie,Otto Hahn Bibl,Pf.2841,37018 Goettingen, on December 5, 2012